

Quantum Interference in Disordered Ferromagnet U_2NiSi_3

D. GNIDA*, M. SZLAWSKA, P. WIŚNIEWSKI AND D. KACZOROWSKI
 Institute of Low Temperature and Structure Research, Polish Academy of Sciences,
 P.O. Box 1410, 50-950 Wrocław, Poland

A single-crystalline sample of disordered ferromagnetic U_2NiSi_3 was investigated by means of electrical resistivity measurements under ambient and high hydrostatic pressure. Temperature dependences of the electrical resistivity clearly reveal interplay of the ferromagnetic ordering and quantum interference effects resulting from crystallographic disorder. Electron–electron interaction manifests itself as a $T^{0.5}$ increase in the in-plane and out-of-plane electrical resistivity below 5 K. Weak localization is observed solely in the ab -plane as a linear-in- T contribution to resistivity, which suggests that internal magnetic field does not break the interference of scattered electron waves in ab -plane. Applied hydrostatic pressure does not affect the $T^{0.5}$ electron–electron interaction contribution, however it diminishes the impact of weak localization on the ab -plane resistivity.

DOI: [10.12693/APhysPolA.127.451](https://doi.org/10.12693/APhysPolA.127.451)

PACS: 72.15.-v, 75.50.Lk, 72.15.Rn

1. Introduction

It is well known that increase in amount of impurities in simple metallic compounds leads not only to increase in residual resistivity but may also result in formation of a low temperature minimum in the electrical resistivity. The origin of this phenomenon was theoretically explained in late seventies [1, 2]. Distinct deviation from the Boltzmann theory has been found in the resistivity behaviour of disordered conductors, which occurs due to interferences between scattered partial electron waves. In order to compensate for that deviation a correction has been introduced that accounts for coherent superposition of wave functions of elastically scattered electrons, called the weak localisation. Such correction is significant if electrons experience multiple elastic scattering on impurities before the constructive interference is destroyed in an inelastic scattering process [2–4]. In addition to that mechanism, electrons moving in a disordered potential may also interact with fluctuating inhomogeneous local electron charge density induced by other electrons, which results in electron–electron interaction correction to the conductivity with the characteristic $T^{0.5}$ dependence [2, 4]. Though both quantum corrections are commonly observed in many disordered conductors, most of the quantitative investigations were limited to simple metallic systems with nonmagnetic ground states.

The main aim of our work was to determine the role of structural disorder in the low-temperature behaviour of the strongly anisotropic ferromagnet U_2NiSi_3 . The compound crystallizes with the AlB_2 -type structure, in which the U atoms occupy the Al(1a) position, while the Ni and Si atoms share the unique B(2d) site. The atomic disorder on the latter site leads to a small value of the residual resistivity ratio (RRR) close to 1 and to an enhanced

residual resistivity, which amounts to about $390 \mu\Omega \text{ cm}$ and $160 \mu\Omega \text{ cm}$ for the electric current flowing perpendicular and longitudinal to the c -axis, respectively [5, 6]. As far as the magnetic properties are concerned, U_2NiSi_3 was characterized in the early literature reports as a spin-glass system with the freezing temperature of 22 K [7] or a re-entrant spin-glass with the ferromagnetic transition at 25 K [8]. Alternatively, it was described as a ferromagnet with the Curie temperature $T_C = 26 \text{ K}$ [9] or $T_C = 30 \text{ K}$ [10]. In the latter study, the polarized neutron diffraction measurement revealed that the uranium magnetic moments of $0.6 \mu_B$ are oriented in the ferromagnetic state perpendicular to the c -axis. Most recently, thermodynamic, electrical transport and neutron diffraction measurements of single-crystalline U_2NiSi_3 confirmed the ferromagnetic ordering below 26 K, with the uranium magnetic moments of $1.05 \mu_B$ [5].

2. Experimental details

High-quality single crystal of U_2NiSi_3 was grown by the Czochralski technique in a tetra-arc furnace under ultra-pure argon atmosphere. Its hexagonal AlB_2 -type crystal structure was confirmed on a four-circle X-ray diffractometer (KUMA Diffraction) equipped with a charge-coupled-device camera, using Mo K_α radiation.

DC magnetic measurements were performed in the temperature interval 1.72–400 K using a superconducting quantum interference device (SQUID) magnetometer (Quantum Design MPMS-5). The results corroborated the ferromagnetic behaviour reported in Ref. [5] and additionally verified the absence of impurity phase $UNiSi_2$ that was observed in our previous study [6].

Four-point AC electrical resistivity measurements were performed from room temperature down to 2 K in hydrostatic pressures up to 2.4 GPa using a PPMS platform (Quantum Design PPMS-9) and a high-pressure clamp cell designed for this equipment (CamCool).

*corresponding author; e-mail: D.Gnida@int.pan.wroc.pl

3. Results and discussion

Figure 1a and b presents the temperature dependences of the resistivity ratios $\rho_c(T)/\rho_c(2\text{ K})$ and $\rho_{ab}(T)/\rho_{ab}(2\text{ K})$ measured on single-crystalline U_2NiSi_3 at ambient pressure and under applied hydrostatic pressure of 2 GPa or 2.4 GPa. As can be inferred from these figures, at ambient pressure the value of RRR amounts only to 1.06 and 0.98 for the in-plane ρ_{ab} and out-of-plane ρ_c resistivity, respectively. In the paramagnetic region, both components change with temperature in similar manner. Upon cooling from 300 K their values decrease to minima placed at 37 K and 45 K, respectively. Further decreasing temperature down to 2 K causes distinct difference in the temperature evolution of the ratio $\rho(T)/\rho(2\text{ K})$. For the current parallel to the hard magnetic axis, $j\parallel c$, the onset of the ferromagnetic state manifests itself in a maximum at $T_C = 27.7\text{ K}$. Then, the $\rho_c(T)/\rho_c(2\text{ K})$ curve displays another minimum located near 10.7 K. On the contrary, no clear anomaly at the magnetic phase transition is observed in the electrical resistivity measured with the current flowing within the hexagonal ab plane. In this case, merely a tiny feature at T_C can be noticed in the temperature derivative of the $\rho_{ab}(T)/\rho_{ab}(2\text{ K})$ variation (see the inset to Fig. 1b).

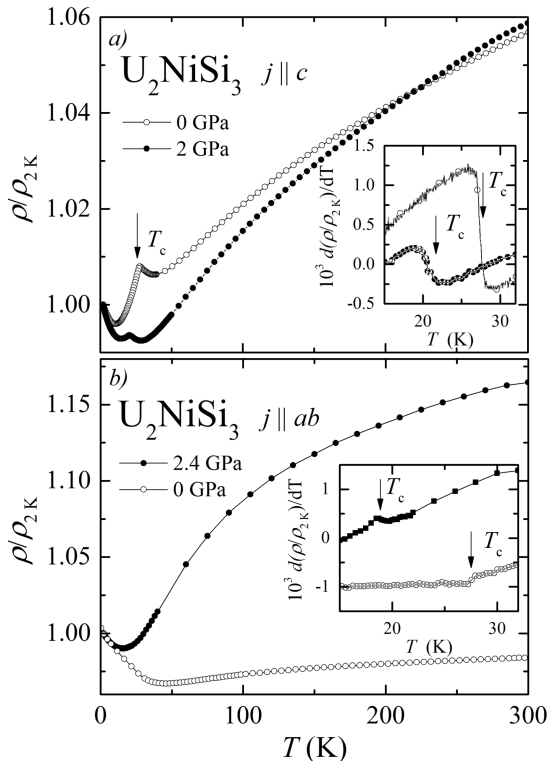


Fig. 1. Temperature dependences of the electrical resistivity ratio $\rho(T)/\rho(2\text{ K})$ of single-crystalline U_2NiSi_3 taken at ambient and applied hydrostatic pressure with the current flowing along the crystallographic c -axis (a) and in the ab -plane (b). The insets show the first derivatives of $\rho(T)/\rho(2\text{ K})$. The arrows indicate the Curie temperature.

From the insets to Fig. 1a and b it is also evident that under pressure the ferromagnetic phase transition shifts to about 20.4 K at 2 GPa and 19 K at 2.4 GPa.

Simultaneously, the minima above T_C shift to 15.5 K for the in-plane and to 28.5 K for the out-of-plane resistivity components. While for the c -axis resistivity the effect of pressure on RRR is very small, RRR of the ab -plane component increases up to 1.16 at 2.4 GPa. Since hydrostatic pressure is not expected to influence elastic mean free path of carriers, the observed change in RRR seems to result from pressure-induced changes in the electronic structure of U_2NiSi_3 .

Figure 2a and b presents the low-temperature $\rho(T)/\rho(2\text{ K})$ data as a function of $T^{0.5}$. Clearly, below about 5 K, the c -axis resistivity can be described as $AT^{0.5}$ with $A = -2.7 \times 10^{-3}\text{ K}^{-1}$ at ambient pressure and $A = -4.1 \times 10^{-3}\text{ K}^{-1}$ at 2 GPa. Similar square-root-of- T dependence is also observed for the in-plane resistivity with the coefficient $A = -5 \times 10^{-3}\text{ K}^{-1}$ being nearly pressure independent. Remarkably, the ab -plane resistivity taken at ambient is proportional to temperature in a wide temperature range 8–25 K (cf. the inset to Fig. 2b).

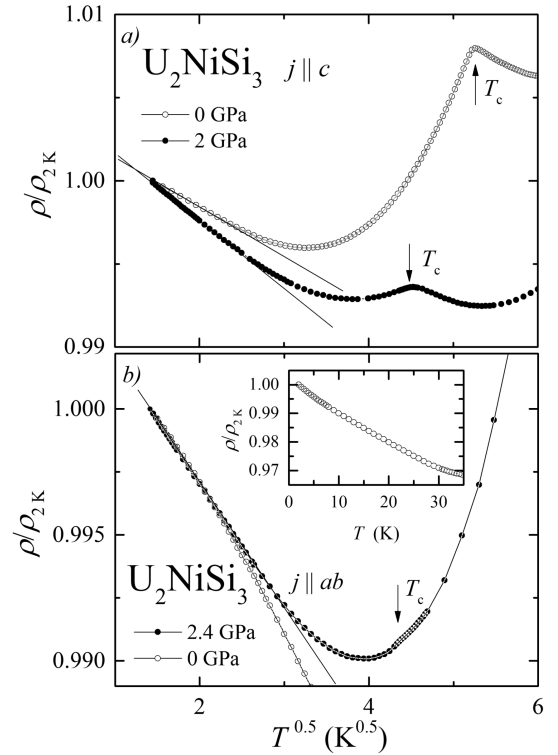


Fig. 2. Electrical resistivity ratio $\rho(T)/\rho(2\text{ K})$ of single-crystalline U_2NiSi_3 plotted as a function of $T^{0.5}$. The data were taken at ambient pressure and under hydrostatic pressure with the current flowing along the crystallographic c -axis (a) and in the ab -plane (b). The arrows indicate Curie temperature. The inset shows a linear-in- T dependence of the ab -plane resistivity.

The observed low-temperature upturns in the $\rho(T)/\rho(2\text{ K})$ curves of U_2NiSi_3 can hardly be attributed to conventional Kondo effect, because strong internal magnetic exchange field in this ferromagnet probably prevents the spins of conduction electrons from flipping under scattering processes. In turn, it seems very unlikely that the low-temperature electrical transport in U_2NiSi_3 can be governed by nonmagnetic Kondo effect, in which conduction electrons interact with an impurity that can change its position in a double well potential. Though such interaction leads to a two-channel non-Fermi liquid behaviour characterized by a $T^{0.5}$ dependence of the resistivity, the characteristic energy scale for Kondo tunnelling was predicted to be very small and the splitting of two lowest energy levels always exceeds T_K [11]. Moreover, it appears that the strong internal magnetic field should break the channel symmetry and consequently destroy the non-Fermi liquid behaviour.

Recently a square-root-of- T increase of the electrical resistivity was found for a cluster-glass compound U_2CoSi_3 that is isostructural to U_2NiSi_3 [12]. The overall temperature and magnetic field dependences of the electrical transport in this material were successfully interpreted by taking into account quantum interference effects, which result from distinct crystallographic disorder. Taking into account the large values of the residual resistivity and the small values of RRR observed for single-crystalline U_2NiSi_3 it seems likely that similar scenario is applicable in the present case. While the electron–electron interaction manifests itself as a $T^{0.5}$ increase in the in-plane and out-of-plane electrical resistivity below 5 K, the weak localization effect is observed solely in the ab -plane resistivity as a linear-in- T contribution to $\rho_{ab}(T)/\rho_{ab}(2\text{ K})$. It implies that internal magnetic field due to exchange interaction does not break the interference of closed trajectories of electrons moving in the ab -plane in opposite directions, similarly to the case of 2D disordered ferromagnets with in-plane magnetic induction [13]. Under hydrostatic pressure one observes an increase of the normal transport resistivity contribution with respect to the quantum correction contribution, which is evidenced by the shift of the resistivity minimum to lower temperatures and by the increase of RRR. As a result, the weak localization effect in the ab -plane resistivity gets suppressed. Surprisingly high pressure hardly affects the electron–electron interaction in the ab -plane resistivity, and the slope of the $T^{0.5}$ upturn increases. Since the diffusion coefficient and the electron–electron interaction constant are directly dependent on the Fermi surface properties, it seems likely that the observed behaviour originates from pressure-induced changes in the electronic structure of U_2NiSi_3 .

4. Conclusions

The low-temperature electrical resistivity of U_2NiSi_3 seems governed by the interplay of ferromagnetism and

quantum interference effects. The resistivity increase proportional to $T^{0.5}$, observed below 5 K, probably results from the electron–electron interaction, and is not destroyed by hydrostatic pressure as high as 2.4 GPa. On the other hand, the weak localization correction, observed below T_C solely in the ab -plane resistivity, gets suppressed under high pressure. This finding suggests that pressure-controlled changes in the electronic structure of U_2NiSi_3 may have a profound influence on the quantum interference effects.

Acknowledgments

We are grateful to Dr. A. Gagor for orienting the single crystals on a four-circle diffractometer. This work was supported by the National Science Centre (Poland) under grants 2011/03/D/ST3/02351 and 2011/01/B/ST3/04482.

References

- [1] E. Abrahams, P.W. Anderson, D.C. Licciardello, T.V. Ramakrishnan, *Phys. Rev. Lett.* **42**, 673 (1979).
- [2] B.L. Altshuler, A.G. Aronov, *Sov. Phys. JETP* **50**, 968 (1979).
- [3] P.A. Lee, T.V. Ramakrishnan, *Rev. Mod. Phys.* **57**, 287 (1985).
- [4] B.L. Altshuler, A.G. Aronov, *Electron–Electron Interactions in Disordered Systems*, Elsevier, Amsterdam 1985.
- [5] M. Szlawaska, D. Kaczorowski, M. Reehuis, *Phys. Rev. B* **81**, 094423 (2010).
- [6] M. Szlawaska, Ph.D. Thesis, INTiBS PAN, Wrocław 2011.
- [7] D. Li, A. Dönni, Y. Kimura, Y. Shiokawa, Y. Homma, Y. Haga, E. Yamamoto, T. Honma, Y. Onuki, *J. Phys. Condens. Matter* **11**, 8263 (1999).
- [8] D. Kaczorowski, H. Noël, *J. Phys. Condens. Matter* **5**, 9185 (1993).
- [9] D.B. Chevalier, R. Pöttgen, B. Darriet, P. Gravereau, J. Etourneau, *J. Alloys Comp.* **233**, 150 (1996).
- [10] D.A. Schröder, M.F. Collins, C.V. Stager, J.D. Garrett, J.E. Greedan, Z. Tun, A.O. dos Santos, A.N. Medina, *J. Magn. Magn. Mater.* **140–144**, 1407 (1995).
- [11] I.L. Aleiner, B.L. Altshuler, Y.M. Galperin, T.A. Shutenko, *Phys. Rev. Lett.* **86**, 2629 (2001).
- [12] M. Szlawaska, D. Gnida, D. Kaczorowski, *Phys. Rev. B* **84**, 134410 (2011).
- [13] V. Dugaev, P. Bruno, J. Barnaś, *Phys. Rev. B* **64**, 144423 (2001).